Electronic Supplementary Information (ESI)

Enhanced Oxygen Reduction Activity on Surface-Decorated Perovskite Thin Films for Solid Oxide Fuel Cells

Eva Mutoro,[a] Ethan J. Crumlin,[a] Michael D. Biegalski,[b] Hans M. Christen,[b] Yang Shao-Horn*[a]

[a]Electrochemical Energy Laboratory, Massachusetts Institute of Technology, 77 Massachusetts Avenue, Cambridge MA 02139,USA, e-mail: shaohorn@mit.edu
[b]Center for Nanophase Materials Sciences, Oak Ridge National Laboratory, Oak Ridge, TN 37831, USA

Index *Page*

Experimental details

Target Synthesis. The $Gd_{0.2}Ce_{0.8}O_2$ (GDC) powder was synthesized via the Pechini method: $Gd(NO_3)_3$ and $Ce(NO_3)_3$ were dissolved into de-ionized water, ethylene glycol, and citric acid (Sigma-Aldrich). After esterification at about 100 °C, the resin was charred at 400 °C and then calcinated at 800 °C for 1 hour in air. The $La_{0.8}Sr_{0.2}CoO_{3-\delta}$ (LSC) powder was synthesized using solid state reaction from a stoichiometric mixture of La_2O_3, $SrCO_3$, and Co_3O_4 (Alfa Aesar) calcinated at 1000 °C for 12 hours in air. The pulsed laser deposition (PLD) targets with a diameter of 25 mm were subsequently formed by uniaxial pressing at 50 MPa and sintered at 1350 °C for 20 hours in air.

The PLD targets for the surface decoration with "La", "Sr", and "Co" phase were prepared from commercial powders, La_2O_3 (Alpha Aesar, 99.99 %), $SrCO_3$ (Alpha Aesar, 99.94 %), and Co_3O_4 (Alpha Aesar, 99.7 %), by uniaxial pressing and sintered at 1100 °C for 23 h in air. The "La" and "Sr" targets have been stored in an Ar flooded glove box (as the materials are hygroscopic and storage in air or in a drying cabinet lead to crack formation and decomposition of the target).

Pulsed Laser Deposition (PLD). 9.5 mol% Y_2O_3-stabilized ZrO_2 (YSZ) single crystalline substrates with (001)-orientation, dimensions 10 x 5 x 0.5 mm, and one-sided polished (surface roughness < 1 nm) (Princeton Scientific) were used as electrolytes (PLD substrates). Before PLD, platinum ink (Pt, #6082, BASF) counter electrodes were painted on the un-polished side of the YSZ and sintered at 800 °C for 1 hour in air. The GDC and LSC oxide films were deposited by PLD using a KrF excimer laser with $\lambda = 248$ nm, $f = 10$ Hz pulse rate, and $E \approx 50$ mJ pulse energy under $p(O_2)$ of 10 mTorr with 500 pulses of GDC (≈3-5 nm) at 550 °C, followed by $N = 15000$ pulses of LSC (≈140 nm, determined by atomic force microscopy (AFM)) at 650 °C. Reflection high-energy electron diffraction (RHEED) was utilized to provide *in situ* monitoring of the GDC and LSC film growth.

Surface decoration ("La", "Sr", "Co") of the films was carried out on micro-patterned LSC films and prepared under the following PLD conditions: $\lambda = 248$ nm, $f = 5$ Hz pulse rate, $E \leq 300$ mJ, $p(O_2) \approx 10$ mTorr, $T_{substrate} \approx 80$ °C, $N = 750$ pulses for "La" and "Co", and for "Sr" 500 pulses (< 4 nm), 750 pulses (< 6 nm), 1000 pulses (≈ 7.5 nm), and 2000 pulses (≈ 15 nm, determined by AFM, see page S5). After the deposition, the samples were cooled to room temperature within the PLD chamber at ≈ 10 mTorr.

Micro-patterning. The LSC microelectrodes were fabricated by photolithography and the following process: OCG positive photo resist (Arch Chemical Co, USA) was applied on the film surface and patterned using a mask aligner (Karl Süss, Germany, $\lambda = 365$ nm). The photo resist was developed using Developer 934 1:1 (Arch Chemical Co., USA), and the films were subsequently etched in hydrochloric acid (HCl) to form ≈ 200 μm circular microelectrodes. The photo resist was removed with acetone. AFM was used to measure sample thickness of the base film (≈ 140 nm). The micro-patterned electrodes were then surface-decorated, as described above. For the "Co" surface decorated sample, the surface decoration on the electrolyte was removed by an additional micro-patterning and acid etching step.

XRD of PLD target materials (for surface decoration)

Figs. S1-S3 show the 2θ-scan (Rigaku) of the target materials (the increased background between $2\theta \approx 55°$ - 75° is an instrumental artifact and was eliminated during data analysis by adjusting the background accordingly). As the material is a mixture of oxide, hydroxide, and carbonate, the diffractogram shows a number of peaks, but all peaks could be assigned to the depicted structures. Using HighScore Plus, a peak profile fit was utilized to determine the ratio of the different phases in each material.

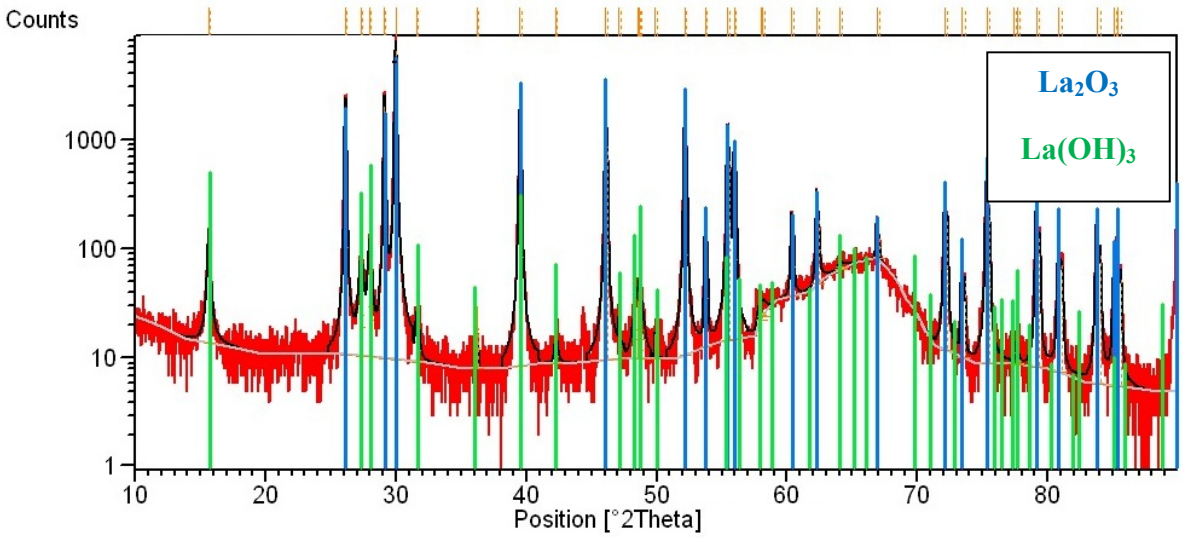

Fig. S1: XRD pattern of the "La_2O_3" target (red: diffractogram, blue: La_2O_3 (98.3 %, reference code: 00-005-0602), green: $La(OH)_3$ (1.7%, reference code: 01-077-3930), black: fitted peaks, grey: background), the small peak at ≈44.5° can be assigned to $La_2(CO_3)O_2$ (with less than 1 %), all other peaks can be assigned to the two La-phases.

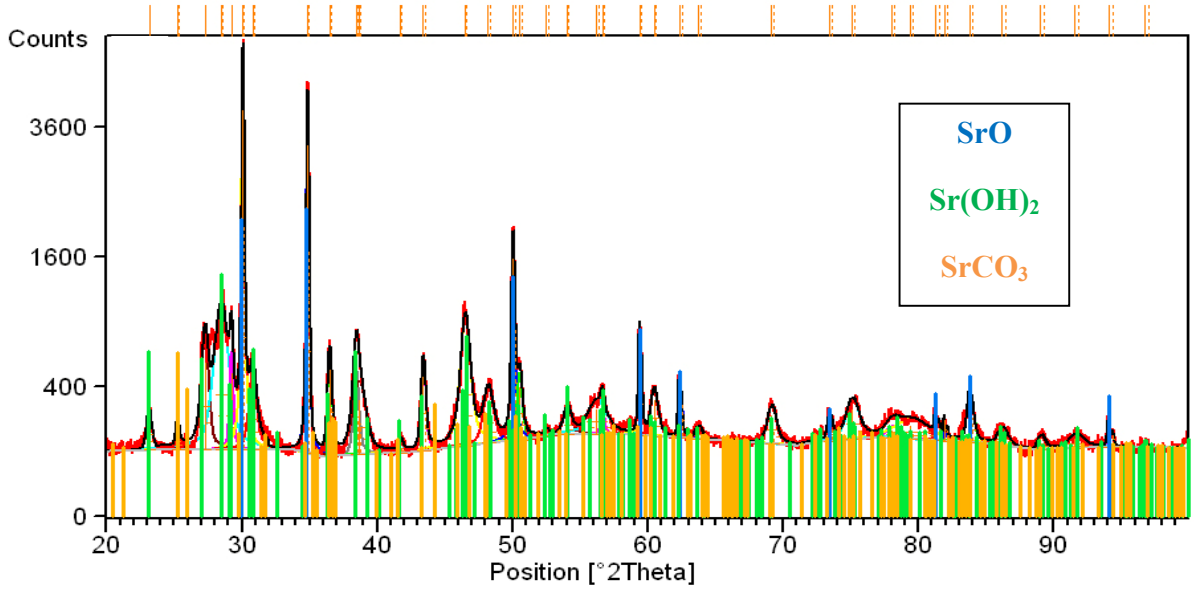

Fig. S2: XRD pattern of the "$SrCO_3$" target (red: diffractogram, blue: SrO (35 %, reference code: 04-006-0780), green: $Sr(OH)_2$ (48 %, reference code: 04-013-8832), orange: $SrCO_3$ (17 %, reference code: 01-071-2393), black: fitted peaks, grey: background), all peaks can be assigned to the three Sr-phases.

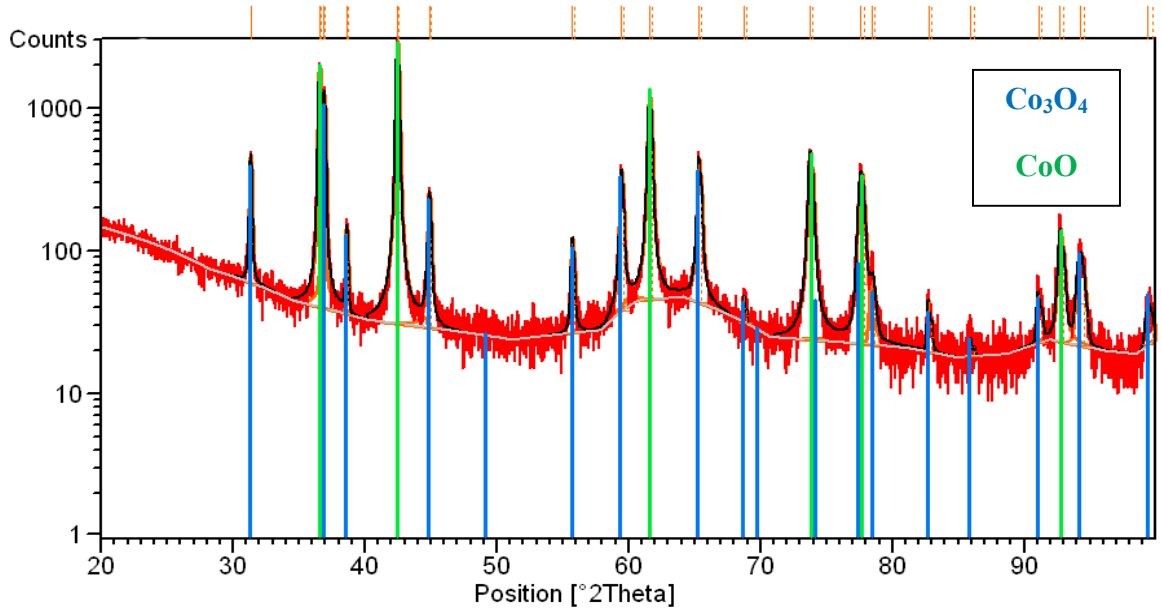

Fig. S3: XRD pattern of the "Co_3O_4" target (red: diffractogram, blue: Co_3O_4 (27 %, reference code: 04-007-8056), green: CoO (73 %, reference code: 01-076-3828), black: fitted peaks, grey: background), all peaks can be assigned to the two Co-phases.

Correlation of "Sr" film thickness after PLD deposition and number of PLD laser pulses

In order to roughly estimate the film thickness of the "Sr" surface decoration, an additional thicker "Sr" layer (2000 pulses) covering half of the surface of a polished YSZ single crystal has been prepared by PLD (identical parameters as for surface decoration). The step height was then determined by AFM, resulting in 15 ± 2 nm. Assuming a linear relationship between number of laser pulses and film thickness results in: 2000 pulses ≈ 15 nm, 1000 pulses ≈ 7.5 nm, 750 pulses < 6 nm, 500 pulses < 4 nm. These values relate to virtual film thicknesses of a "Sr" film after PLD and before heat treatment/EIS testing (and not to the height of the particles formed on the LSC surface).

Information on the electrochemical testing and analysis

Electrochemical characterization. Samples were placed on a substrate with an Ag mesh and fixed to this mesh using Ag ink. The counter electrode was contacted with a mircoprobe tip on the Ag mesh, while another mircoprobe tip was used to contact the center of the micro-cathodes. The sample was heated to a temperature of 510 °C (measured with a thermocouple on the sample surface) and tested with EIS under Ar / O_2 mixtures in the range from $p(O_2)$ of 1 atm to 10^{-4} atm (starting at the highest oxygen partial pressure).

Data analysis. By fitting the EIS data to the equivalent circuit shown in **Fig. 2b**, $R_{electrolyte}$-($R_{electrolyte/electrode\ interface}$/$CPE_{electrolyte/electrode\ interface}$)-($R_{ORR}$/$CPE_{ORR}$), we obtained values for R_{ORR}; knowing the area of the microelectrode ($A_{electrode}$ = 0.25 π $d_{electrode}^2$, with $d_{electrode}$ = 200 µm) we can determine the electrical surface exchange coefficient (k^q) utilizing this expression:[1] $k^q = RT / 4F^2 R_{ORR} A_{electrode} c_o$, where R is the universal gas constant (8.314 J mol^{-1} K^{-1}), T is the absolute temperature (783 K), F is Faraday's constant (96,000 C mol^{-1}),

and c_o is the lattice oxygen concentration in LSC. In a first approximation, we estimated c_o for LSC using: $c_o = (3–\delta) / V_m$, where V_m is the bulk molar volume of LSC at room temperature (33.66 $cm^3 \cdot mol^{-1}$; increasing the temperature to 510 °C has a negligible effect on V_m). Oxygen nonstoichiometry, δ values, for LSC at the experimental conditions (p, T) have been used from literature. We used the values for LSC for the unmodified base film and the surface decorated samples. Admittedly, the surface decoration might change the c_o value of the system. However without exactly knowing the active phase on the surface, a reasonable estimation is impossible. Assuming e.g. the Ruddlesden-Popper Phase $LaSrCoO_{4\pm\delta}$ to be the active material, we could use the following expression: $c_o = (4+\delta) / V_m$ for a pure $(La,Sr)_2CoO_{4\pm\delta}$ surface, with V_m of bulk $LaSrCoO_{4\pm\delta}$ at room temperature (54.60 cm^3 mol^{-1}). The influence of using the $(La,Sr)_2CoO_{4\pm\delta}$ c_o would increase the value of k^q by approximately 20 %. We decide to use c_o values of LSC for all (surface-decorated) samples for a better comparison and as this is also the larger c_o value and will yield in the most conservative k^q values.

AFM details

General image processing. Image processing of all depicted AFM images included: flattening and selecting a height scale of 100 nm ('black = 0 nm' to 'white = 100 nm' in the images) using Nanoscope software; converting the image into gray scale and coloring (still having black correlating to 0 nm and white to 100 nm) using Adobe Photoshop CS4 extended.

Additional AFM images. **Fig. S4** shows AFM images of the base LSC film **a**) microelectrode surface before EIS testing, and **b**) microelectrode surface after EIS testing. The surface morphology after EIS testing of the base film differs from the "La", "Sr", and "La" decorated surfaces after EIS testing (**Fig. 4b**): the features on the base film surface are comparably flat (height ≈ 15 nm) leading only to a marginal increase in the surface area (by factor of 1.02). **Fig. S4c** depicts the surface of a base film (5 x 5 mm) after PLD decoration with 1000 pulses before temperature treatment/EIS testing. The surface is completely covered with a "Sr" particle film. After heat treating this sample (**Fig. S4d**), the morphology changed and larger particles formed (surface not completely covered by particles any more). The depicted morphology is similar to the surface of "Sr" decorated microelectrodes after EIS testing (**Fig. 4b**). **Fig. S4e** shows the surface of the sample with 2000 laser pulses of "Sr" after EIS (insulating film). The entire surface is covered with particles, and nearly no uncovered film surface is remaining.

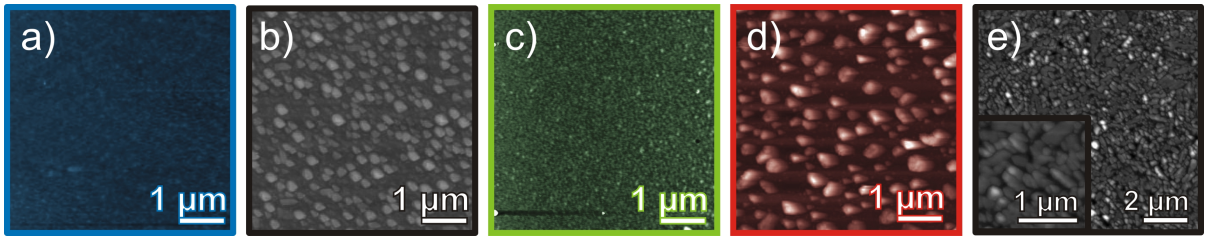

Fig. S4: a) Representative AFM image of base LSC surface before EIS testing (microelectrode), and b) after EIS testing (microelectrode); a 1000 laser pulse "Sr"-decoration (5 mm x 5 mm film) c) before and d) after heat treatment, e) the 2000 laser pulse "Sr"-decoration after EIS (microelectrode). The maximum height (white) of all images is 100 nm.

Image analysis. The RMS roughness and the real surface areas have been determined using the AFM Nanoscope software. **Tab. S1** and **Fig. S5** summarize the obtained values of representative 100 μm^2 AFM images:

Sample	Number laser pulses surface decoration	Temperature treatment (510 °C) / EIS	RMS roughness / nm	Surface area / μm^2
Ideally flat	**0**	-	**0**	**100.00**
Base film	0	no	0.62	100.02
Base film	0	yes	9.21	102.16
Sr decorated (< 4 nm)	500	yes	13.66	106.51
Sr decorated (< 6 nm)	750	yes	11.80	104.94
Sr decorated (≈ 7.5 nm)	1000	yes	19.15	105.90
Sr decorated (≈ 7.5 nm)	1000	no	11.41	103.14
Sr decorated (≈ 15 nm)	2000	yes	1.73	100.22
La decorated	750	yes	9.02	100.64
Co decorated	750	yes	14.50	102.13

Table S1: Summary of different RMS values and surface areas of the surfaces (100 μm^2 AFM images)

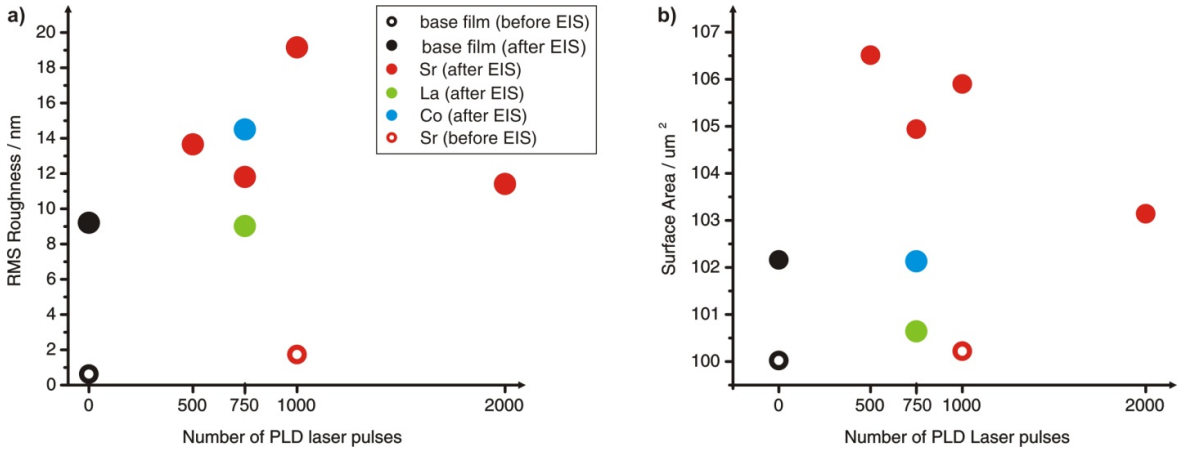

Fig. S5: Plot of a) the RMS roughness of different surfaces, and b) the surface area versus the number of PLD laser pulses; filled circles represent surfaces after heat treatment/EIS, while unfilled circles correspond to surfaces after PLD preparation.

The coverage of particles, particle-free film area, and the perimeter of the surface particles have been determined using Adobe Photoshop CS4 extended. **Fig. S6** depicts the 750 pulse-"La" surface after testing and the selected areas (particles in white) used for determining the area covered by particles. The large spherical particles (**Fig. S6a**) cover 2.75 % of the area; selecting in addition also smaller particles (**Fig. S6b**) results in 3.64 % coverage.

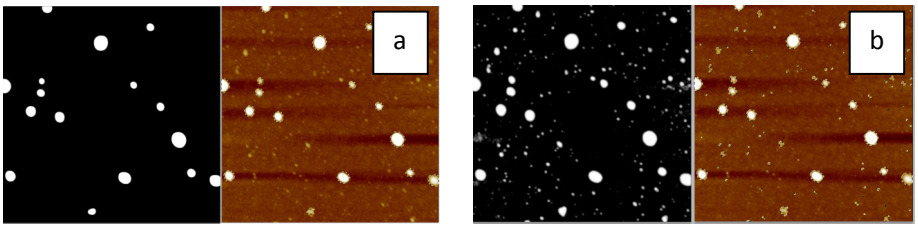

Fig. S6: Selected area (white) and correlating AFM image, a) large particles: 16 particles covering 2.75 % area (tpb length/area: 24.27 μm^{-1}); large and smaller particles: 102 particles covering 3.64 % area (tpb length/area: 53.49 μm^{-1}). Note: tpb length is defined as the perimeter of the particles.

For the "Sr"-decorated surfaces the area covered by particles, the particle-free area, and a perimeter length of the particles has been determined selecting the areas shown in **Fig. S7**. Particles are marked in black. The results are summarized in **Tab. S2**. As the films have been characterized *ex situ* after EIS testing, the morphology may correlate to the k^q values measured at lowest oxygen partial pressure. Thus **Fig. S8** depicts the average k^q values for the three "Sr" coverages at 1000 ppm O_2 versus different morphology characteristics.

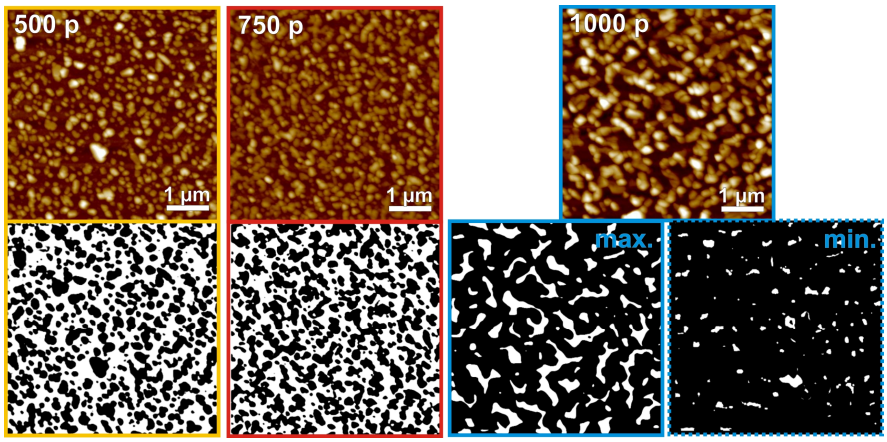

Fig. S7: AFM images (5 um x 5 um) and the corresponding areas selected for image analysis (black = particle, white = particle-free surface). For the 1000 pulses (7.5 nm) sample it is harder to determine the particle-free surface, and thus two estimations (min. and max.) have been made (the minimum estimation marked with a dotted line is less likely).

"Sr" decorated sample	Surface decoration / laser pulses	*T* treatment (510 °C) / EIS	Coverage of Particles / %	Particle-free surface / %	Perimeter of particles on a 25 µm^2 area
< 4 nm	500	yes	50.0	50.0	92
< 6 nm	750	yes	50.8	49.2	245
≈ 7.5 nm	1000	yes	80.0 (-95.2)*	4.8-20.0*	50-110*
* minimum and maximum values, see Fig. S7					

Table S2: Summary of determined morphology characteristics of the Sr decorated surfaces

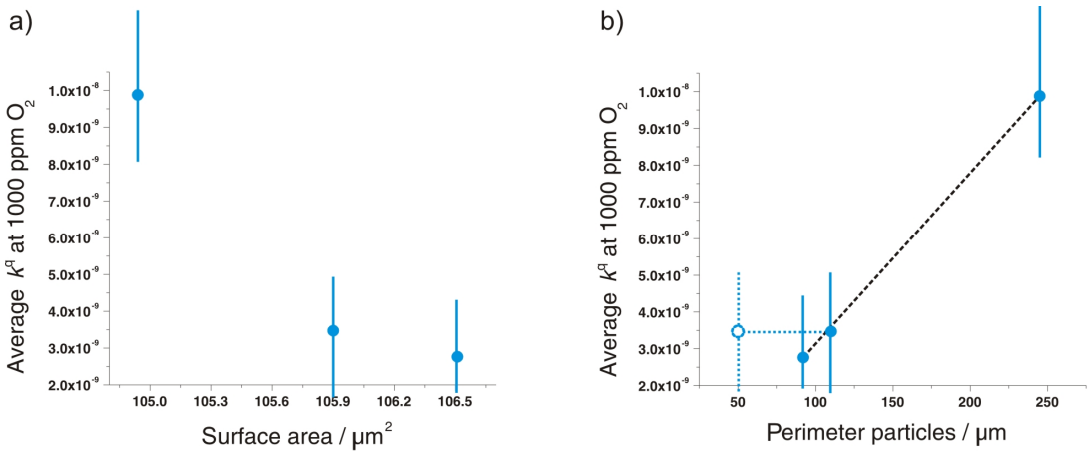

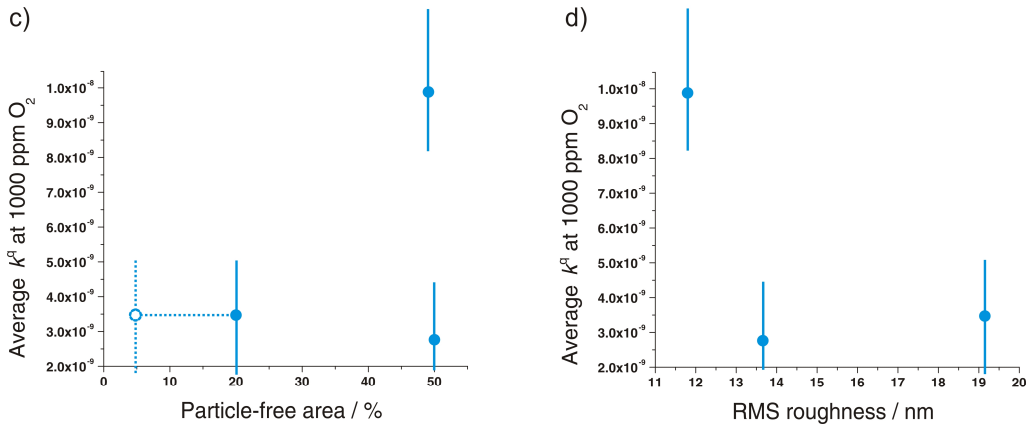

Fig. S8: Plots of k^q values (average value marked with a circle, range marked with a bar) versus selected morphology characteristics (the dotted lines represent the minimum estimation, see **Fig. S7**); a) surface area, b) perimeter of particles, c) no correlation to particle-free area (also no correlation to particle coverage, not shown), and d) rms roughness. Not depicted: no correlation to number of laser pulses.

As there are only three data points available, any trend has to be treated with caution. Obviously there is no correlation between surface the exchange coefficient and number of laser pulses, surface roughness, area covered with particles, nor the particle-free area. A dependency of the surface exchange coefficient with the particle-free surface area would be expected if Sr dissolving in LSC was the main factor for the observed k^q enhancement. Interestingly, the highest k^q value was found on the sample with smallest surface area. This result suggests that not the entire surface area is active for ORR. Furthermore, the data indicate a linear relationship between the perimeter of the particles (defined as the line between the black and the white areas in **Fig. S7**). This correlation is in agreement with the hypothesis of having a catalytically active reaction phase at the interface between the insulating particles and the LSC film.

XPS details

Literature values. Reviewing literature values[2-4] for La $3d_{5/2}$, Sr $3d_{5/2}$, O 1s, and Co $2p_{3/2}$ for LSC, and the La-, Sr-, and Co- oxides, hydroxides and carbonates, the binding energies typically vary over a range of a few eV, if reliable XPS data are available. Comparing peak positions in literature, even the expected E_{bind} trends based on the nearest-neighbors electronegativity argument (initial state effect), e.g. E_{bind}(metal) < E_{bind}(metal oxide), are not always reflected. One reason for this lack of precise literature reference data is the challenge to collect XPS of some of the pure materials as they easily react e.g. with H_2O or CO in the air. The peak positions for e.g. $SrCO_3$, $Sr(OH)_2$, and SrO are overlapping (**Tab. S3**),[4] and thus it is impossible to distinguish between these phases based on the peak positions.

Peak fitting. For peak fitting CasaXPS was utilized. The smallest number of components was used to obtain a reasonable fit, despite the fact that some peaks are known to consist of a number of unresolved overlapping components (e.g. Sr 3d after "Sr"-decoration is composed of a $SrCO_3$, $Sr(OH)_2$ and a SrO peak, or the C1s carbonate peak is composed of more than one carbonate species). We did not use additional unresolved components for fitting (e.g. 5 components for O 1s or 3 components for Sr 3d of LSC) as proposed by Van der Heide[3]–despite the fact that a good fit could be obtained with this approach. Therefore a slightly larger fwhm of all peaks composed of more than one component was chosen compared to peaks only assigned to a single component (e.g. O^{2-} in 'lattice/bulk' LSC). In general, identical fwhm's for doublets and (nearly) identical for

all components of peaks of one element have been chosen. Peak assignment, peak, and satellite positions, and doublet separations are based on literature values; relative intensities of doublet pairs are considered (2:1 for p electrons and 3:4 for d electrons). A Shirley background was utilized; peaks are described as convolution of Gaussian and Lorentzian function. Due to the fact that some (surface related) peaks are composed of more than one component, a small peak shift might be due to a different ratio between these components (and not a chemical shift of one component). **Tab. S3** details all peaks, peak assignments, and the binding energies.

				unmodified LSC film		LSC + 1000 pulses "Sr"		LSC + "Sr" + *T*		
Peak		**Assignment (ref. values E_{bind} / eV)**		**E_{bind} / eV**	**Atom %**	**E_{bind} / eV**	**Atom %**	**E_{bind} / eV**	**Atom %**	**Comments**
C1s		adventitious C (≈ 248.6 – 285.0[5])		285.0	-*	285.0	-*	285.0	-*	Spectra shifted to C1s (adventitious carbon) = 285 eV[5]
C1s		carbonate (≈ 288.7 - 290)[3]		288.7	23.2	289.2	12.7	288.8	23.7	Carbonate always assigned to surface
La 3d	5/2, 3/2	5/2: LSC surface (835.3-837.7)[3, 6], 5/2: LSCF 834.7,[3] LSCGO/LSFGO 834.5[3]		834.7, 851.5	11.9	NA	NA	834.1, 850.9	2.8	Overlapping between La lattice and La surface, thus atomic percentages may have larger error than for other elements.
	5/2, 3/2	5/2: LSC lattice (833.4[7]-833.7)[3], LSCF 833.0[3]		832.9, 849.8.	21.2	NA	NA	832.5, 849.3	16.9	
	sat.: 5/2, 3/2	ΔE_{bind} ≈ 3.8-3.9,[8] 4.0[3]	LSC surface	838.2, 855.3		NA	NA	837.9, 854.6		
			LSC lattice	836.7, 853.6		NA	NA	836.4, 853.2		
Sr 3d	5/2, 3/2	5/2: LSC surface (133.0-133.1, 134-134.2),[3, 7] $SrCO_3$(133-133.1)[4], SrO(133-135.5)[6], $Sr(OH)_2$(133.2)[4]		133.7, 135.4	5.0	132.9, 134.6	28.2	133.2, 135.0	14.9	Surface related peak is composed of three components, thus larger fwhm compared to LSC lattice peak
	5/2, 3/2	5/2: LSC lattice (130.5[7]-132)[3, 7]		131.6, 133.3	6.0	NA	NA	131.4, 133.0	10.1	
Co 2p	3/2, 1/2	3/2: LSC lattice (≈ 780.0-780.5,[6] 780.6[3])		779.6, 794.9	14.0	NA	NA	779.5, 795.0	10.9	Co assigned completely to LSC lattice as peak fit does not allow separation in lattice and surface; typically perovskite show surface carbonates or Sr/A-site enrichment[3, 9-17]
	sat.: 3/2, 1/2	LSC lattice		789.3, 803.7		NA	NA	789.2, 803.4		
O 1s		LSC surface (530-533.4),[3] $SrCO_3$(531.3-531.7)[4], SrO(530.3[6]-530.7),[4] $Sr(OH)_2$ (531)[4]		531.5	60.0	530.9	59.1	531.2	58.5	Surface related peak is composed of at least three components, thus larger fwhm compared to LSC lattice peak
		SiO_2 or $Sr(NO_3)_2$ (532.3[18] - 534.0[19] /534[20])		NA	NA	533.5	-*	533.6	-*	Impurity (SiO_2 or $Sr(NO_3)_2$ not expected to be ORR active)
		LSC lattice (528.5[7]-528.7[3])		528.4	58.7	NA	NA	528.1	62.0	

Table S3: Binding energies (eV) and atomic percentages (%) of the elements C, La, Sr, Co, and O from XPS spectra of the LSC base film, the LSC film after depositing 1000 laser pulses "Sr", and after heat treatment. Peaks assigned to the surface of the sample are marked blue, lattice LSC peaks green. * = not included in percentage calculation. Peak positions of literature values relate to C1s (adventitious carbon) = 285 eV.

Estimation of Sr diffusion in LSC

The diffusion coefficient for Sr ions in LSC is rather low at 510 °C, therefore Sr enrichment would be limited most likely to the outermost surface. Assuming Sr diffusion is comparable in different perovskites[21] and an extrapolation to lower temperature is valid, one can very roughly estimate a diffusion length $\Delta x_{diff} = (2 \cdot D \cdot t_{diff})^{1/2}$. For bulk material ($D_{bulk}^{510\ °C} \approx 1.6 \cdot 10^{-23}$ cm^{-2}·s^{-1},[21] t_{diff} = 4 h) virtually no diffusion takes place ($\Delta x_{diff} = 2.2 \cdot 10^{-12}$ m), but assuming grain boundary diffusion ($D_{gb}^{510\ °C} \approx 3.9 \cdot 10^{-17}$ cm^{-2}·s^{-1},[21] t_{diff} = 4 h) the diffusion length is $1.1 \cdot 10^{-8}$ m. Only assuming a surface having some defects in the outermost layer(s), the diffusion coefficient may be larger than the bulk value, and Sr diffusion into LSC cannot be completely excluded.

ESI References

1. J. Maier, *Physical Chemistry of Ionic Materials: Ions and Electrons in Solids* John Wiley, Chichester, England ; Hoboken, NJ, 2004.
2. C. D. Wagner, Naumkin, A. V., Kraut-Vass, A., Allison, J. W., Powell, C. J., Rumble Jr, J. R. , National Institute of Standards and Technology (NIST), 2003, vol. Version 3.5
3. P. A. W. van der Heide, *Surf Interface Anal*, 2002, **33**, 414-425.
4. R. P. Vasquez, *Journal of Electron Spectroscopy and Related Phenomena*, 1991, **56**, 217-240.
5. D. Briggs, Seah, M. P., ed., *In Practical Surface Analysis*, Wiley, New York, 1983.
6. A. E. Bocquet, P. Chalker, J. F. Dobson, P. C. Healy, S. Myhra and J. G. Thompson, *Physica C*, 1989, **160**, 252-258.
7. A. Galenda, M. M. Natile, V. Krishnan, H. Bertagnolli and A. Glisenti, *Chem Mater*, 2007, **19**, 2796-2808.
8. Y. A. Teterin, A. Y. Teterin, A. M. Lebedev and K. E. Ivanov, *Journal of Electron Spectroscopy and Related Phenomena*, 2004, **137**, 607-612.
9. H. Dulli, P. A. Dowben, S. H. Liou and E. W. Plummer, *Phys Rev B*, 2000, **62**, 14629-14632.
10. P. Decorse, E. Quenneville, S. Poulin, M. Meunier, A. Yelon and F. Morin, *J Vac Sci Technol A*, 2001, **19**, 910-915.
11. T. T. Fister, D. D. Fong, J. A. Eastman, P. M. Baldo, M. J. Highland, P. H. Fuoss, K. R. Balasubramaniam, J. C. Meador and P. A. Salvador, *Appl Phys Lett*, 2008, **93**, 151904.
12. R. Bertacco, J. P. Contour, A. Barthelemy and J. Olivier, *Surf Sci*, 2002, **511**, 366-372.
13. P. Decorse, G. Caboche and L. C. Dufour, *Solid State Ionics*, 1999, **117**, 161-169.
14. Q. H. Wu, M. L. Liu and W. Jaegermann, *Mater Lett*, 2005, **59**, 1480-1483.
15. J. A. Marcos, R. H. Buitrago and E. A. Lombardo, *J Catal*, 1987, **105**, 95-106.
16. S. Fearn, J. Rossiny and J. Kilner, *Solid State Ionics*, 2008, **179**, 811-815.
17. V. I. Sharma and B. Yildiz, *J Electrochem Soc*, 2010, **157**, B441-B448.
18. D. Sprenger, H. Bach, W. Meisel and P. Gutlich, *Journal of Non-Crystalline Solids*, 1990, **126**, 111-129.
19. I. Montero, L. Galan, E. Delacal, J. M. Albella and J. C. Pivin, *Thin Solid Films*, 1990, **193**, 325-332.
20. A. B. Christie, J. Lee, I. Sutherland and J. M. Walls, *Appl Surf Sci*, 1983, **15**, 224-237.
21. T. Horita, M. Ishikawa, K. Yamaji, N. Sakai, H. Yokokawa and M. Dokiya, *Solid State Ionics*, 1998, **108**, 383-390.